2005

Using Incongruent Equilibrium Hydration Reactions to Model Latter-Stage Crystallization in Plutons: Examples from the Bell Island Tonalite, Alaska

J. S. Beard

P. C. Ragland

Maria Luisa Crawford
Bryn Mawr College, mcrawfor@brynmawr.edu

Custom Citation

Beard, J. S., P. C. Ragland, and M. L. Crawford (2005) Using incongruent equilibrium hydration reactions to model latter-stage crystallization in plutons: Examples from the Bell Island Tonalite, Alaska, *J. Geol.*, 133, 589-599.

Using Incongruent Equilibrium Hydration Reactions to Model Latter-Stage Crystallization in Plutons: Examples from the Bell Island Tonalite, Alaska

James S. Beard,[1] *Paul C. Ragland, and Maria L. Crawford*[2]

Virginia Museum of Natural History, 1001 Douglas Avenue, Martinsville, Virginia 24112, U.S.A.
(e-mail: jbeard@vmnh.net)

ABSTRACT

Models using hydration crystallization reactions (the reverse of dehydration melting reactions such as amph + qtz = px + melt) for the Bell Island pluton define incongruent equilibrium crystallization paths from hydrous melt + pyroxene + Fe-Ti oxides + calcic andesine (30%–50% solid) to a solid tonalite consisting mostly of hornblende, biotite, epidote, sodic andesine, and quartz. In essence, hydration crystallization is a way to quantify and modify the lower temperature end of Bowen's discontinuous reaction series and apply it to natural samples. Hydration crystallization provides an alternative to crystal fractionation for explaining variations in pluton chemistry, especially the compositions of late plutonic melts. Another characteristic of hydration crystallization is that the reactions have the potential to buffer the water content of the melt during crystallization. Two closed-system models, representing different sets of starting conditions and phases, are considered, based on least squares, mass-balance calculations of reactions and constrained by the petrography of the rocks. Model 1 starts with an average modified Bell Island leucotonalite melt coexisting with two pyroxenes, two Fe-Ti oxides, and plagioclase at the beginning of hydration crystallization. The starting assemblage of model 2 omits orthopyroxene and magnetite, includes amphibole, and uses a calculated melt composition. Both models generally predict, via different series of hydration crystallization reactions, the observed subsolidus mode. Model 2, however, is preferred based on petrographic observations of the Bell Island rocks, specifically the lack of magnetite and orthopyroxene, as well as certain textural features.

Online enhancement: appendix.

Introduction

A wide variety of amphibole- and biotite-bearing rocks undergo incongruent melting to yield hydrous, silicic melts coexisting with an anhydrous mineral assemblage (dehydration melting; Thompson 1982; Beard and Lofgren 1991; Rushmer 1991; Wolf and Wyllie 1994; Patino Douce and Beard 1995, 1996; Rapp 1995; also see the review by Vielzeuf and Schmidt [2001]). These reactions are reversible and vapor absent (Thompson 1982; Patino Douce and Beard 1995, 1996). Beard et al. (2004) have proposed that the reverse of incongruent dehydration melting occurs during the cooling and solidification of hydrous magmas. They termed this reverse process "hydration crystallization." Reaction stoichiometry, the temperature at which melting/crystallization begins, and the temperature range over which the reactions occur vary according to bulk composition of the system. Pressure also has an effect, expanding the stability field of hydrous minerals and (at pressures of >7–10 kbar) sometimes producing garnet as a part of the anhydrous solid assemblage (Patino Douce and Beard 1996; Vielzeuf and Schmidt 2001). Most reactions involving amphibole have the general form (written here in the hydration crystallization form and garnet free)

$$\text{hydrous (tonalite) melt} + \text{pyroxene} + \text{Fe-Ti oxides} \pm \text{calcic plagioclase} = \text{amphibol} + \text{quartz} \pm \text{sodic plagioclase},$$

Manuscript received September 20, 2004; accepted April 5, 2005.

[1] Author for correspondence.

[2] Bryn Mawr College, Bryn Mawr, Pennsylvania 19010, U.S.A.

[The Journal of Geology, 2005, volume 113, p. 589–599] 0022-1376/2005/11305-0006$15.00

and, for biotite,

hydrous (granite) melt + pyroxene
+ Fe-Ti oxides ± calcic plagioclase
= biotite + quartz ± sodic plagioclase.

At pressures of 5–10 kbar, these reactions typically occur at temperatures between 850°C (lower for some Fe-rich biotites) and 950°C (e.g., Patino Douce and Beard 1995; Vielzeuf and Schmidt 2001). Although the crystallization of amphibole and/or biotite late in the solidification history of hydrous plutons is essentially universal, there have been few attempts to quantify the process. We use hydration crystallization reactions to provide a template for describing the genesis of hydrous minerals during the cooling and solidification of a hydrous magma as an equilibrium, incongruent crystallization process.

The Bell Island Pluton

The Bell Island pluton is a 90-Ma, 1300-km^2 epidote-biotite-hornblende tonalite pluton that is largely homogeneous in three dimensions at the kilometer scale. It is a component of the mid-Cretaceous continental arc exposed in southeast Alaska and northwest British Columbia (Crawford et al. 1987; Gehrels and Berg 1994; Rubin and Saleeby 2000; fig. 1). Along most of its margin, the pluton intrudes early Paleozoic to mid-Mesozoic metasedimentary and metavolcanic rocks. *PT* estimates from contact aureole assemblages suggest that the pluton is tilted. Estimated pressures of emplacement from the northern and western parts of the pluton are in the range of 6–7 kbar; those from the south and east range from 8 to more than 10 kbar (Cook and Crawford 1994). This interpretation is consistent with amphibole chemistry and the occurrence of garnet within the pluton (Cook 1991; Cook and Crawford 1994). Temperatures (based on dehydration melting equilibria) were likely in the 850°–950°C range during amphibole and biotite formation. The pluton is truncated along its eastern margin by a major Eocene structure, the Coast Shear Zone (Cook and Crawford 1994).

The pluton consists of coarse-grained (up to 10 mm), hypidiomorphic granular biotite-hornblende tonalite with minor granodiorite and quartz diorite. It is cut by leucocratic granodioritic to granitic dikes and pegmatites (much less common in the core of the pluton) and contains locally abundant enclaves of gabbroic and dioritic material. More weakly defined mesoscale heterogeneities include

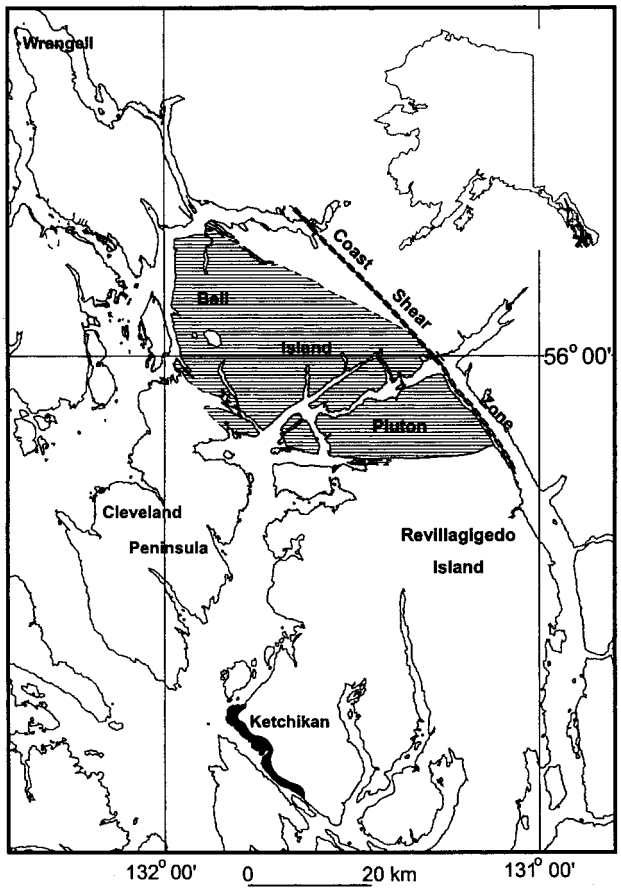

Figure 1. Location and outline of Bell Island pluton. Local geology modified after Gehrels and Berg (1994).

diffuse centimeter-scale modal layering and schlieren defined by concentrations of mafic or felsic minerals. The pluton is weakly zoned, with a somewhat more leucocratic core. A strong, linear fabric, defined by aligned plagioclase and mafic minerals, is present in most samples. This fabric, which plunges east at a low angle, appears to be an igneous flow fabric, possibly developed during emplacement (Cook and Crawford 1994; Crawford et al. 2002). Some samples, particularly those from the eastern margin in the vicinity of the Coast Shear Zone, also show evidence for subsolidus deformation (e.g., idiomorphic granular texture, especially in quartz). Alteration is generally mild and manifested by nonpervasive, dusty, sericitic alteration of plagioclase and chloritization of biotite. In a few more strongly altered samples, there is substantial saussuritization of plagioclase and chloritization of all mafic phases.

Igneous Mineralogy. Plagioclase is the most abundant phase (modal average about 45%) in the

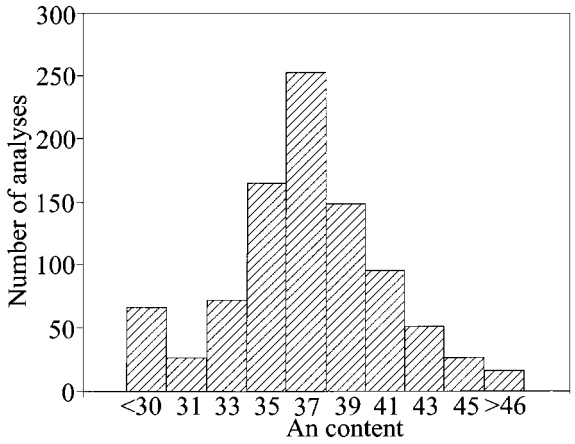

Figure 2. Frequency distribution of plagioclase analyses from the Bell Island pluton. Most rims are An_{33} or less; most cores are An_{40} or more. This distribution is used to constrain the plagioclase composition and mode throughout the hydration crystallization models.

pluton. It occurs as weakly to moderately zoned, complexly twinned, tabular to equant subhedral crystals. Most grains have a small, irregular core of calcic andesine ($An_{42–47}$, rarely to An_{53}) mantled by a thick, continuously zoned andesine ($An_{32–39}$) rim. Many grains have an outermost sodic rim ($An_{7–30}$). The frequency distribution of plagioclase compositions determined by microprobe analysis is shown in figure 2. This distribution is used to define the plagioclase modes and compositions for the hydration crystallization models. Plagioclase grains in contact with K-feldspar usually have an albitic and/or myrmekitic rim. Perthite and/or tartan-twinned K-feldspar (microcline) occurs in about half of the Bell Island samples. In most samples, it is a minor, interstitial phase but constitutes 10%–20% of several samples from near the pluton's core.

Quartz makes up about 20% of the Bell Island pluton. Habits include interstitial, symplectitic with biotite or epidote, dispersed grains within amphibole, and, in a few samples from the center of the pluton, large, blocky grains. Most quartz is strained but only weakly recrystallized. In a few more strongly deformed samples, subgrain and even granular textures are developed, but these are uncommon.

Amphibole (15% of the pluton by mode) is a brownish- or bluish-green ferroan pargasitic hornblende (Leake 1978). The amphibole is weakly zoned, with rims enriched in K, Al, and Fe. Calcic, Ti-, and Al-poor augite ($Mg_{\#63–69}$) occurs as remnant cores in amphibole in several samples from near the western and southern margins of the pluton.

Biotite (approximately equal in abundance to amphibole) occurs as anhedral to subhedral dark reddish-brown crystals. They have compositions (moderate Al and Fe contents) typical of biotite from hornblende-bearing granitoids (Speer 1984). The biotite has experienced subsolidus reequilibration at high temperature (e.g., to low-Ti biotite) and is also locally chloritized. High Ti (average 3.3 wt% TiO_2) biotite is taken as approximating the igneous composition.

One to three percent igneous epidote/clinozoisite ($Clz_{25–65}$) occurs in most Bell Island samples. Epidote occurs as overgrowths on allanite, as anhedral to blocky subhedral crystals associated with biotite and amphibole, and as symplectic intergrowths with quartz or biotite. The symplectites usually occur at the margins of blocky allanite or epidote crystals. Subsolidus Fe-epidote occurs in altered plagioclase and biotite or with calcite and other alteration minerals.

Allanite occurs in almost every sample. Allanite is almost always surrounded by a rim of igneous epidote having rare earth element below microprobe detection limits. Traces of ilmenite occur in most samples as inclusions in plagioclase, pyroxene, amphibole, and, rarely, quartz. Pyrrhotite is the commonest opaque phase, and partial oxidation of pyrrhotite to hematite is common, especially in more altered samples. Magnetite has not been identified in any sample.

Order of Crystallization. The earliest crystallizing phases in the Bell Island pluton are plagioclase (sodic labradorite or calcic andesine preserved in the cores of zoned plagioclase) and augite (now preserved only as remnants within amphibole). Plagioclase crystallization continued throughout the solidification history, but, as we will argue below, augite entered a reaction relationship with the melt to produce amphibole, quartz, and biotite. Amphibole and quartz crystallization commenced relatively early, after plagioclase and augite but before

Table 1. Starting Modes for Crystallization Models

	Plag	Opx	Cpx	Mt	Ilm	Amph	Melt	Plagioclase composition
Model 1	33.5	9.8	6.3	.9	1.1	0	48.4	An_{39}
Model 2	17.1	0	5.1	0	1.2	5.4	71.3	An_{41}

Table 2. Actual and Calculated Subsolidus Modes

	Plag	Amph	Bio	Ep	Sph	Qtz	Ksp	Ilm	Cpx
Point count[a]	47	15	14	1.7	Trace	20	2.4	Trace	Trace
Least squares[b]	46	19	11	.6	.0	18	4.9	.0	.0
Model 1	46	20	10	1.1	.1	18	4.4	.2	.0
Model 2	46	19	11	1.1	.0	18	4.5	.2	.0

[a] Average of 46 point counts of Bell Island pluton tonalite thin sections recast as a wt% mode; 400–500 points per section, ~20,000 total points counted.
[b] Least squares mode calculated using average mineral compositions to reconstruct the average bulk composition of the Bell Island pluton.

biotite, sphene, allanite, or epidote. Allanite is always overgrown by epidote. Quartz, plagioclase, amphibole, and biotite continued to crystallize through most of the solidification history, although in some samples amphibole appears to enter a reaction relationship with biotite late in the crystallization sequence. The latest crystallizing phases are sodic plagioclase (usually $An_{15–25}$), quartz, and K-feldspar, along with epidote, sphene, and biotite.

Hydration Crystallization Models for the Bell Island Pluton

We present two models using incongruent hydration crystallization reactions to define a crystallization path, starting with a hydrous melt in equilibrium with an anhydrous mineral assemblage (±amphibole) and resulting in a solid in which mafic minerals are dominantly or entirely hydrous. We have chosen the models to represent two different sets of starting conditions and phases. Other mathematically valid models, most of which involved reaction of large amounts of plagioclase with hydrous melt, were discarded for lack of petrographic evidence of such reactions. Model 1 uses a modified average Bell Island pluton leucotonalite to represent the melt composition coexisting with two pyroxenes, two Fe-Ti oxides, and plagioclase at the onset of hydration crystallization (table 1).

Table 3. Bulk, Mineral, and Melt Compositions Used in the Crystallization Models

	SiO_2	TiO_2	Al_2O_3	MgO	CaO	MnO	FeO	Na_2O	K_2O
Bulk composition (average Bell Island pluton):									
Average BIP	59.97	.71	17.15	2.79	5.88	.12	5.77	3.59	2.09
Minerals:									
Amph, high-Mg	42.97	1.10	12.85	9.08	11.76	.45	16.96	1.25	1.41
Amph, core	42.85	1.18	12.43	8.61	11.69	.45	18.04	1.28	1.33
Amph, rim	42.18	1.05	13.50	8.15	11.68	.44	18.2	1.29	1.41
Biotite	36.33	3.44	16.72	9.48	.03	.30	19.91	.10	8.81
Epidote	37.72	.22	27.05	.03	23.61	.16	7.59		
Quartz	100.00								
K-feldspar	63.22		18.63		.01		.02	.95	15.46
Opx[a]	50.26	.16	3.13	16.36	1.76	.76	27.10		
Augite	52.16	.05	.79	11.39	23.65	.68	10.94	.31	
Mt							100.00		
Ilm	.03	51.05	.02	.11	.18	3.33	44.72		
Sphene	30.10	38.63	1.94		28.86		.45		
An_{18}	63.20		22.48		3.73			9.51	.12
An_{34}	60.02		25.00		7.05		.04	7.54	.16
An_{37}	58.61		25.87		7.60		.04	7.15	.17
An_{39}	57.94		26.01		8.09		.04	6.96	.15
An_{41}	57.49		26.52		8.48		.05	6.77	.16
Melts:[b]									
1start	68.61	.35	16.12	.94	3.22	.05	2.41	3.24	3.94
1rxn2	72.76	.14	14.73	.37	2.10	.02	.95	3.57	4.38
2start	65.02	.04	17.07	2.37	3.79	.05	5.48	2.40	2.77
2rxn2	66.65	.04	16.54	2.03	3.37	.04	4.68	3.29	3.35
2rxn3	70.90	.02	14.85	1.14	1.95	.02	2.64	2.26	6.23

[a] Bulk composition is the average of 42 chemical analyses of Bell Island pluton tonalites and excludes mafic enclaves and late felsic differentiates. All mineral compositions are from the Bell Island pluton except for opx (Deer et al. 1963, p. 19, analysis 16) and magnetite (assumed to be mt_{100}), neither of which currently occur in the pluton.
[b] Melt compositions are numbered by model. For example, 1start is the initial melt composition for model 1, 2rxn2 is the evolved melt composition used in calculations in model 2 for reaction 2, and so forth.

Table 4. Crystallization Models

Models and reactions	Output
Model 1:[a]	
Reaction 1: cpx, mt out, $\Sigma r^2 = .02$	33.7 melt + 6.3 cpx + 4.2 opx + .88 mt + .21 ilm > 19.6 hbl core + 8.34 An_{18} (melt) + 6.77 K-spar (melt) + 7.56 qtz (melt) + 2.93 qtz
Reaction 2: opx out, $\Sigma r^2 = .44$	18.45 melt 2 + 5.7 opx + 0.57 ilm > 1.99 hbl rim + 7.91 biotite + 8.69 qtz + 6.12 An_{18}
Reaction 3: melt out, $\Sigma r^2 = .00$	18.93 melt 2 + 1.11 hbl rim + .09 ilm > 1.65 biotite + 1.08 epidote + 6.15 qtz + 4.41 K-spar + 6.81 An_{18} + .06 sphene
Model 2:[b]	
Reaction 1: An_{37} crystallization, $\Sigma r^2 = .00$	34.8 melt + 2.92 cpx + .45 ilm > 8.21 hbl core + 4.35 biotite + 12.7 An_{37} + 2.71 K-spar (melt) + 1.46 An_{18} (melt) + 2.09 qtz (melt) + 6.61 qtz
Reaction 2: An_{34} crystallization, $\Sigma r^2 = .00$	34.6 melt 2 + 2.01 cpx + .42 ilm > 5.78 hbl rim + 4.50 biotite + 13.3 An_{34} + 4.05 K-spar (melt) + 0.21 An_{18} (melt) + 2.13 qtz (melt) + 7.01 qtz
Reaction 3: cpx, melt out $\Sigma r^2 = .00$	14.5 melt 3 + .16 cpx + .17 ilm + .48 hbl rim > 2.23 biotite + 1.07 epidote + 4.50 qtz + 4.45 K-spar + 3.00 An_{18}

Note. For all models, initial plagioclase composition and the amount and composition of plagioclase produced during crystallization is constrained by the plagioclase distribution shown in figure 2. A detailed discussion of how these least squares models were formulated is given in the appendix available in the online edition or from the *Journal of Geology* office.

[a] No plagioclase reaction, no plagioclase crystallization at the onset of hydration crystallization, melt allowed to vary. Initial melt is modified BIP leucotonalite.

[b] Continuous plagioclase crystallization and melt evolution during crystallization. Initial melt composition calculated from known plagioclase and assumed mafic mode.

In order to use this melt composition to reconstitute the bulk composition of the Bell Island pluton at the onset of hydration crystallization, two phases (orthopyroxene and magnetite) that do not at present occur in the pluton must be incorporated into model 1. Model 2 incorporates only solid phases (amphibole, augite, plagioclase, and ilmenite) that occur in the pluton (table 1). The melt composition at the onset of hydration crystallization for model 2 is derived by mass balance. Both models reproduce, via a series of hydration crystallization reactions, subsolidus modes that are consistent with point count data for the Bell Island pluton (table 2). Ultimately, evaluation of these models is largely dependent on how well each model reproduces petrographic and petrologic observations.

Assumptions and Constraints for Reaction Modeling. The reaction models for the Bell Island pluton are for a closed system, based on least squares mass balance and constrained by crystallization history and the distribution and abundance of minerals in the rock. For details of the procedure used to formulate the models, see the appendix, available in the online edition or from the *Journal of Geology* office. The models are constrained by the following information: (1) a mineral mode based on the average of 46 point-counted thin sections (average 400–500 points per section, ~20,000 total points; table 2); (2) major-element chemical analyses of the pluton (average of 42 whole-rock analyses of Bell Island pluton tonalites, excluding mafic enclaves and leucocratic differentiates) and its constituent phases (table 3); and (3) a knowledge, based on petrography, of the crystallization history of the pluton, especially reaction/resorption relationships. The underlying assumptions are (1) the magma composition is approximated by the average whole-rock, major-element composition of the Bell Island pluton (table 3). Note that this assumption makes no claims as to whether this magma represents an original liquid composition or a liquid with accumulated crystals. (2) Early in its crystallization history, the Bell Island pluton magma consisted of a liquid plus augite, plagioclase, and ilmenite with orthopyroxene and magnetite (model 1) or amphibole (model 2).

The melt composition for model 1 is taken as an average of several analyses of silicic rocks, including late dikes and silicic segregations, from the Bell Island pluton. Because of high alkali residuals, the Na/K ratio of this composition was adjusted downward by increasing K and decreasing Na while keeping total alkalis approximately constant. Arguably, this compensates for near- or subsolidus alkali mobility, an effect commonly observed in granitoid and, especially, tonalitic plutons (e.g., Drummond et al. 1986). In fact, it is also a serious weakness of model 1, as will be discussed below. In principle, the use of orthopyroxene and magnetite in model 1 can be justified on the basis of melting and crystallization experiments (especially dehydration

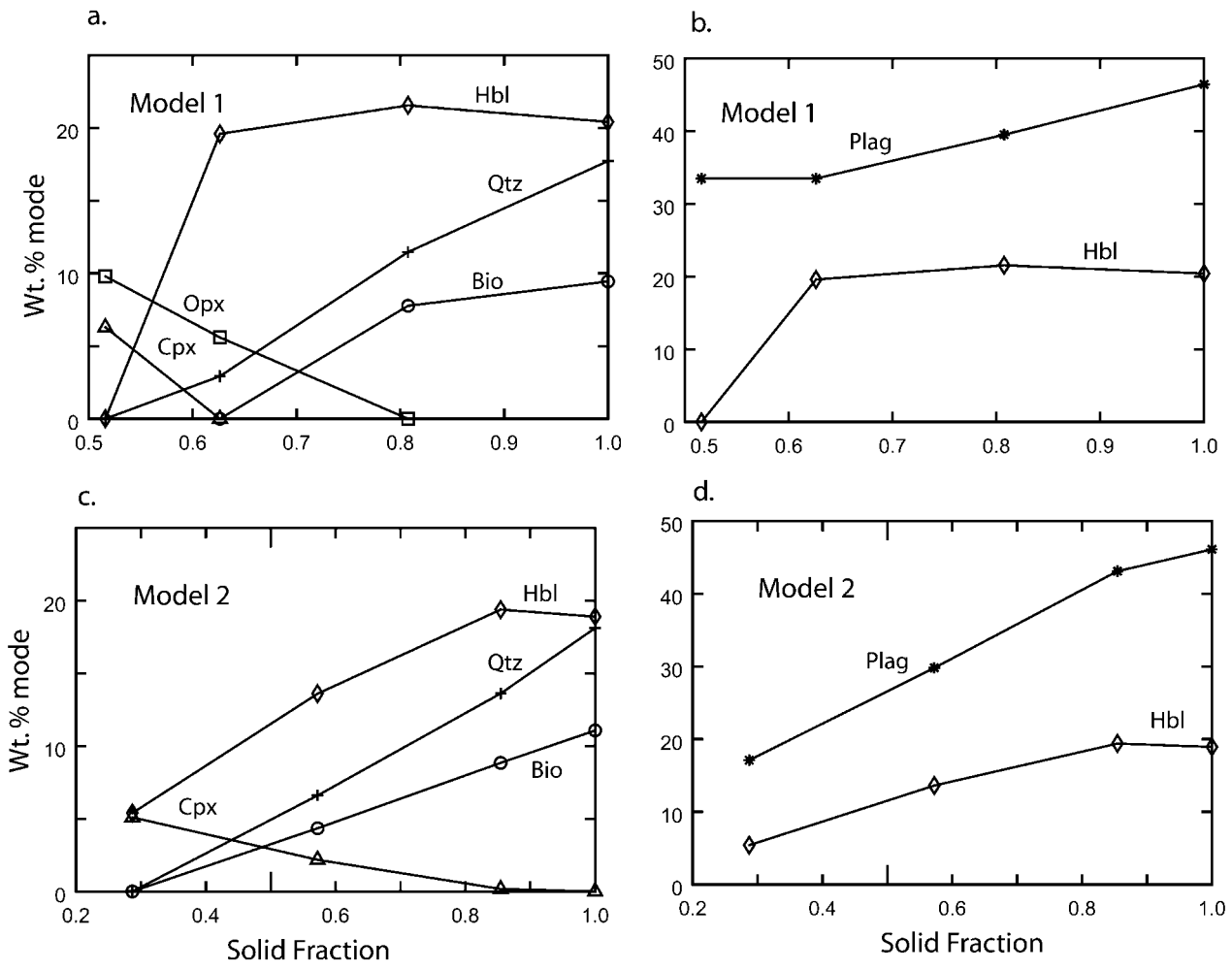

Figure 3. Results of the crystallization model. *a*, Change in solid mode during crystallization, model 1. *b*, Variation in plagioclase and amphibole mode during crystallization, model 1. *c*, Change in solid mode during crystallization, model 2. *d*, Variation in plagioclase and amphibole mode during crystallization, model 2.

melting experiments; e.g., Vielzeuf and Schmidt 2001) and the abundance of these phases in natural andesites and dacites. It may also be that pyrrhotite, which is common in the pluton, acts as an iron donor/sink in place of magnetite. Pyrrhotite cannot be directly used in modeling because there are no whole-rock sulfur data for the pluton. The orthopyroxene composition used in model 1 is from a two-pyroxene dacite (Deer et al. 1963; table 3). For the purposes of model 1, the magnetite is assumed to be mt_{100}. The composition and mode of plagioclase used in the model are based on point count and microprobe data (fig. 2; table 2).

Model 2 has amphibole, augite, plagioclase, and ilmenite coexisting with melt at the onset of hydration crystallization. All of these minerals are present in the Bell Island pluton. The initial mode and composition of plagioclase (17% An_{41}) in the model is based on point count and microprobe data (fig. 2; table 2). The initial mode chosen for augite (5%) is bracketed on the low end by the presence of up to 2% relict augite in some samples and on the high end by the observation that models starting with >8% modal augite ultimately fail to reproduce the subsolidus mode. The model is relatively insensitive to the amount of amphibole present at the onset of hydration crystallization; valid models can be constructed with amphibole modes ranging from 0% to 10%. A median value of 5% was chosen to reflect the likely early crystallization of amphibole in this hydrous, high-pressure system (Cook and Crawford 1994). The

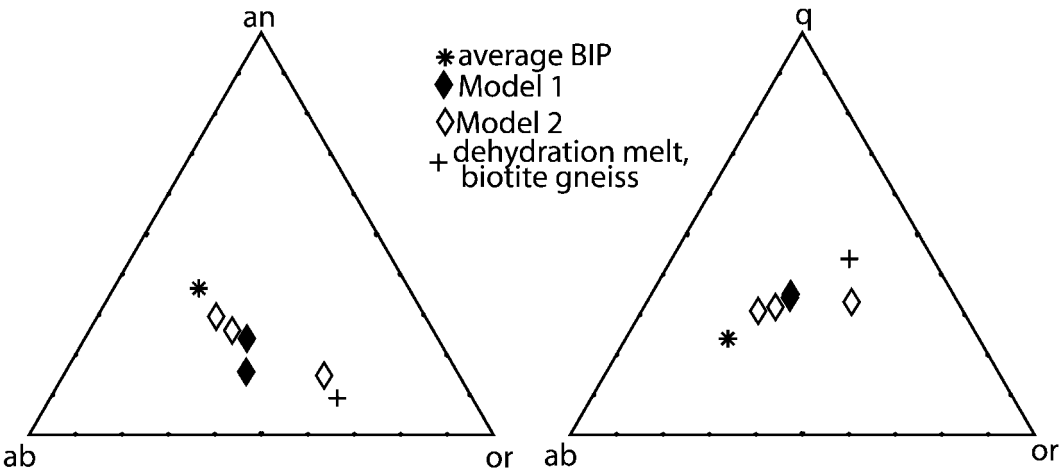

Figure 4. Plots of normative feldspar and quartz for model melts. Melts in model 1 show some increase in total alkali feldspar. Melts generated by model 2 define a clear trend between the bulk rock composition (average Bell Island pluton) and a typical dehydration melt (7 kbar, 900°C; Patino Douce and Beard 1995) in equilibrium with biotite, feldspar, quartz, and pyroxene.

ilmenite mode (~1%) is close to a maximum, constrained by the abundance of Ti in the bulk composition. The composition of the initial solid assemblage (plagioclase + cpx + amphibole + ilmenite) is subtracted from the bulk composition (i.e., the average composition of Bell Island pluton tonalite; table 3) and the result normalized to 100% to yield the melt composition used in the model.

Evolution of the Melt Composition during Reaction. Many of the reactions in table 4 have potassium feldspar and sodic plagioclase as product phases. Because both of these phases are known from petrography to be among the last to crystallize in the Bell Island pluton, their presence as reaction products early in the crystallization sequence is interpreted to signal a change in melt composition. The evolution of the melt composition during reaction is modeled by adding the two feldspars and quartz, such that the ratio of total feldspar to quartz is 2 : 1 by weight ("haplogranite"), back into the melt remaining after the reaction. This modified melt composition is then used in the subsequent reaction. See appendix for a more detailed explanation.

Model 1. In model 1, three reactions define a path from an initial assemblage containing 48% melt coexisting with an anhydrous mineral assemblage (table 1) to a solid hornblende-biotite-epidote tonalite (tables 2, 4). It can be seen from crystallization diagrams (fig. 3) that the first reaction produces a large quantity of amphibole, largely by reaction of augite with melt, with relatively little solidification. This reaction results in the complete consumption of both augite and magnetite without crystallization of plagioclase. The second reaction is orthopyroxene out and results in the crystallization of 8% biotite and sodic plagioclase. Epidote, potassium feldspar, and sphene join the crystallizing assemblage during final solidification. Melt compositions evolve toward slight alkali feldspar enrichment (fig. 4).

Model 2. In model 2 the initial assemblage contains 71% melt (table 1). Three reactions also define crystallization of this system. Unlike model 1, crystallization of plagioclase plays an early and important role in the hydration reactions. In reaction 1, substantial plagioclase crystallizes from the melt concurrently with augite consumption and hornblende and biotite production (fig. 2). Note that both the amount and composition of plagioclase produced by this model are constrained by microprobe and modal data (fig. 2; table 2). Plagioclase, hornblende, and biotite continue to co-crystallize throughout most of the modeled crystallization sequence. Epidote and potassium feldspar are, again, late crystallizing phases. Melt compositions evolve toward both quartz and K-feldspar enrichment and approach the composition of dehydration melts that coexist with biotite, pyroxene, feldspar, and quartz (Patino Douce and Beard 1995; fig. 4).

Discussion

Bowen's Discontinuous Reaction Series Extended to Natural Examples. In essence, hydration crystallization is an attempt to quantify the lower temperature end of Bowen's discontinuous reaction se-

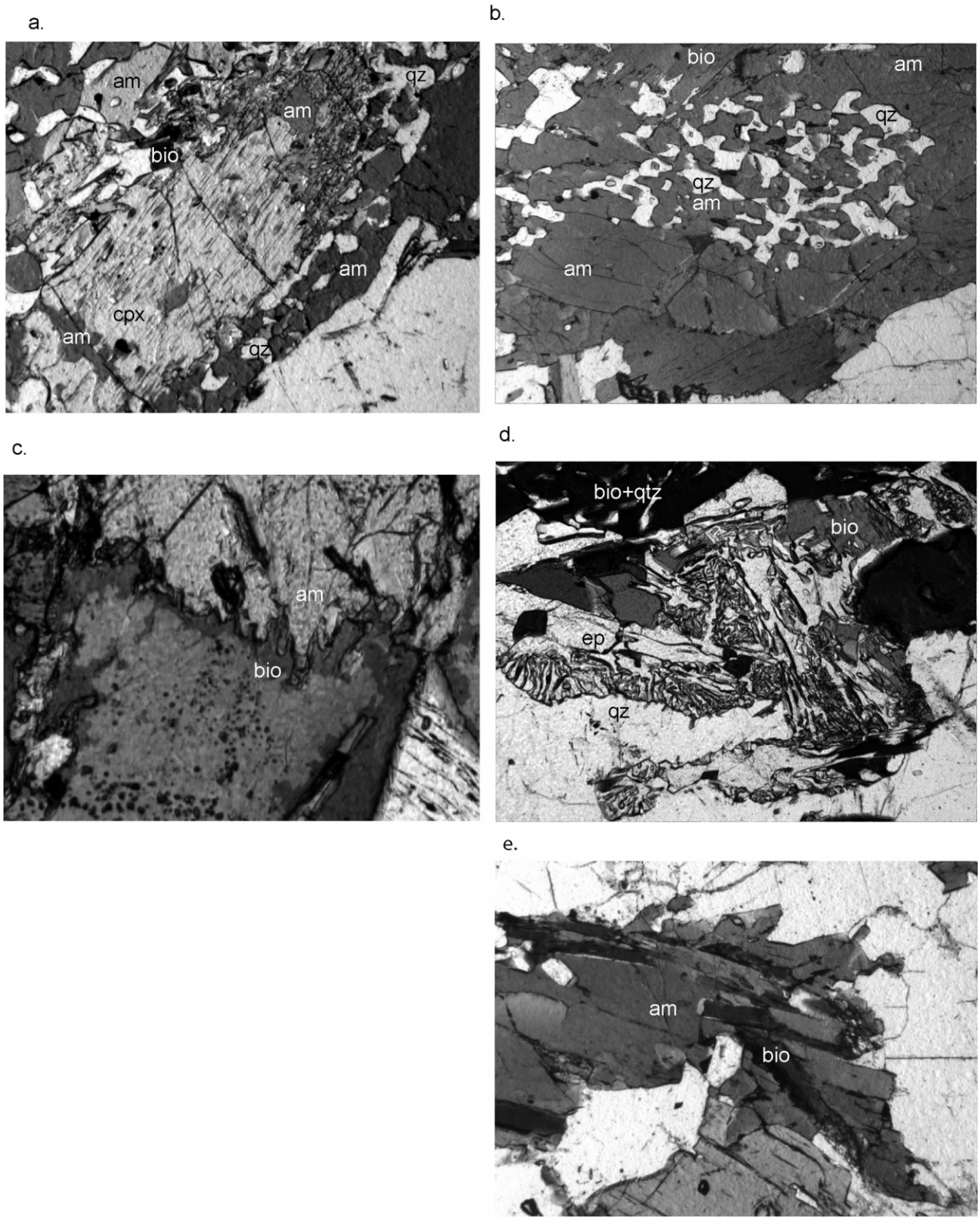

Figure 5. *a*, Augite in reaction (hydration crystallization) relationship with amphibole. Note the presence of minor biotite in the reaction assemblage and the association of quartz with amphibole in the reaction corona. Field of view 3 mm. *b*, Quartz-amphibole intergrowth in the core of a blocky amphibole. This texture is a relict of the augite hydration reaction. Field of view 3.5 mm. *c*, Biotite replacing amphibole. This texture is very rare in the Bell Island

ries and apply it to natural examples. Textures suggesting the replacement of pyroxene by amphibole and biotite are familiar to anyone who has examined a calc-alkaline plutonic suite in thin section. Most would agree that these are reaction textures and are, in fact, the observational basis for the lower temperature end of the discontinuous reaction series (Bowen 1928). Although the replacement, for example, of clinopyroxene by amphibole is far from isochemical, we are unaware of any prior attempt to model quantitatively the reaction process and gauge its influence on magma genesis and evolution.

Evaluation of the Models. Both models are consistent with several key aspects of Bell Island pluton petrography. Both require a reaction relationship between melt and augite to produce hornblende and biotite (fig. 5*a*). Both models predict early co-crystallization of quartz and amphibole as part of the hydration crystallization process (fig. 5*b*). Both predict late co-crystallization of epidote, quartz, and biotite and a late (and relatively minor) reaction relationship between amphibole and biotite (fig. 5*c*, 5*d*). Both also imply that late crystallization of the pluton occurred at temperatures below 950°C and possibly at temperatures as low as 800°C (e.g., Vielzeuf and Schmidt 2001). Several observations and the overall evaluation of assumptions suggest to us, however, that model 2 best describes hydration crystallization in the Bell Island pluton.

The primary apparent advantage of model 1 versus model 2 is the use of an extant rock composition for the initial melt in the model. However, although it may be justified on the basis of alkali mobility, the necessary adjustment of the Na/K ratio in this melt to make the model functional can be construed as considerably weakening this advantage. In principle, there is no reason why the melt present at the onset of hydration crystallization should be preserved in the pluton at all. On the other hand, the necessity of using solid phases not present in the pluton may be seen as a considerable flaw in model 1. This is particularly true because the model predicts that augite, which is present in small amounts in the pluton, will react out before orthopyroxene, which is not present. If the amphibole-forming reaction is a distributary reaction akin to those postulated by Helz (1981) and Sisson and Grove (1993), the disparity between the early modeled demise of clinopyroxene and its occasional preservation in pluton is even more troubling. Finally, model 1 predicts that almost all of the amphibole forms over a very narrow solidification interval (fig. 3) and that it predates biotite crystallization. Although biotite appears to have begun to crystallize later than amphibole in most samples, textures consistent with significant co-crystallization of hornblende and biotite are also common (fig. 5*e*). In fact, biotite appears to partially replace augite in many samples, although it is never as abundant a replacement mineral as amphibole (fig. 5*a*).

Despite the fact that the initial melt composition in model 2 is a least squares construct, the model appears to reproduce both initial conditions and crystallization paths more realistically than model 1. First, the model does not require use of solid phases not currently present in the Bell Island pluton; amphibole + augite is a reasonable high-pressure mineral assemblage in rocks of Bell Island pluton composition (Vielzeuf and Schmidt 2001). Second, the plagioclase mode and composition in the model is constrained by modal and chemical data initially and throughout the solidification history. Although model 2 predicts that amphibole will crystallize before biotite, it also allows for substantial co-crystallization and even involvement of biotite in the clinopyroxene-consuming reactions. All of these observations are consistent with petrographic observation. The end-stage crystallization of two feldspars is also consistent with observation, although, as is typical of plutonic feldspars, late feldspars in the Bell Island pluton do not preserve their high-temperature ternary character. Melts predicted by model 2 evolve toward typical 5–10-kbar dehydration melts of biotite-bearing rocks (fig. 4). Given that crystallization processes modeled here are the reverse of dehydration melting, evolution toward these melt compositions is exactly what one expects in the late stages of a system in which biotite is forming by reaction of melt and pyroxene.

Magma Genesis and Volatile Behavior. One char-

rocks, consistent with the predictions of both models, especially model 2. Field of view 0.6 mm. *d*, Late, near solidus symplectic intergrowths of epidote, biotite, and quartz. Field of view 1.7 mm. *e*, Intergrown amphibole and biotite. Although much amphibole crystallization predates biotite, textures like this suggest significant co-crystallization, consistent with the predictions of model 2. Field of view 2 mm.

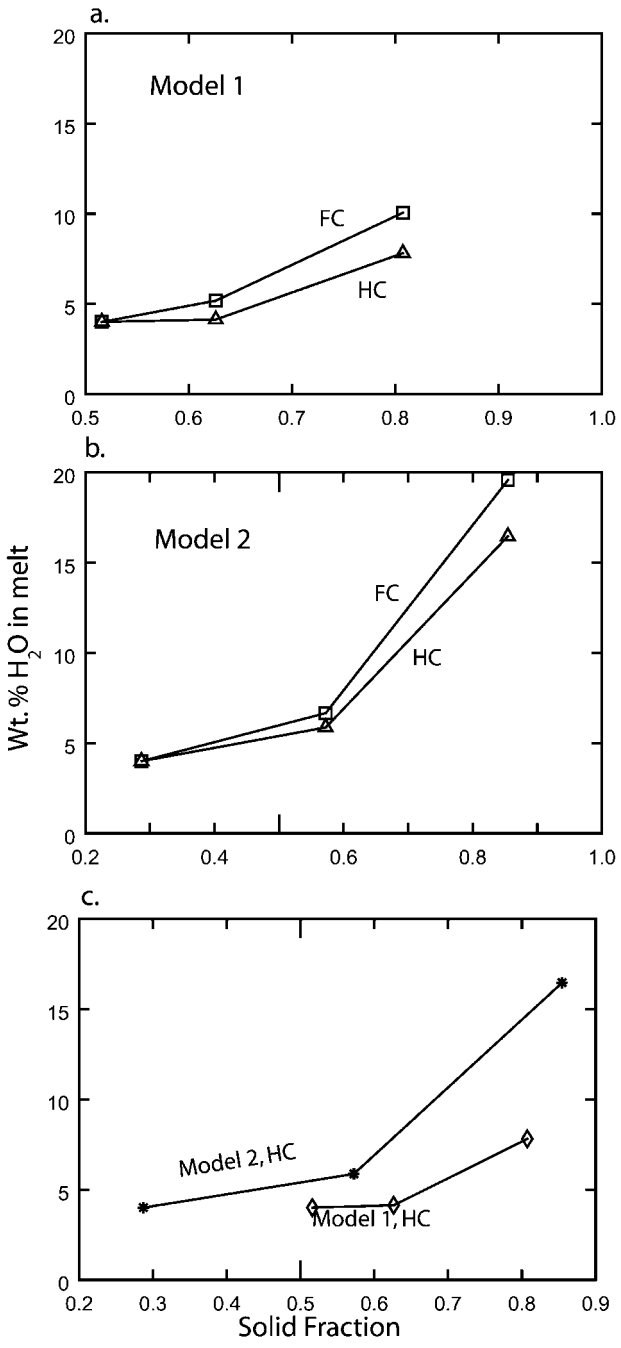

Figure 6. Calculated water concentration in melt during crystallization. Comparison of water concentration change during hydration crystallization versus Rayleigh fractionation of the same hydrous assemblage for model 1 (*a*) and model 2 (*b*). *c*, Comparison of water behavior during hydration crystallization for the two models. Water concentration in the melt at the start of hydration crystallization is set at 4%. Amphibole and epidote are assumed to contain 2 wt%, biotite 4 wt% water. All other phases are assumed to be anhydrous.

acteristic of hydration crystallization reactions is that they have the potential to buffer the water content of the melt during crystallization. If hydration crystallization occurs at a low-variance peritectic, the potential exists for complete crystallization of a hydrous melt to occur without achieving water saturation (Beard et al. 2004). For complex systems such as the Bell Island tonalite, this is not likely to be the case. Nevertheless, even in systems as complex as the Bell Island pluton, hydration crystallization reactions have implications for the behavior of water in the melt. In particular, given identical initial melt fractions and water contents, the formation of a hydrous mineral assemblage by reaction between anhydrous minerals and melt will always result in a lower melt water content than the crystallization of that same assemblage directly from the melt (fig. 6; Beard et al. 2004). Note, however, that the models predict that the melts will eventually become water saturated.

Hydration crystallization, an equilibrium, incongruent process, provides an alternative to crystal fractionation for explaining late-stage variations in pluton chemistry. These evolved equilibrium melts are likely to be important in understanding the origin of late magmatic liquids including aplites, pegmatites, and melt inclusions in late crystallizing phases (e.g., zircon; Thomas et al. 2002). For example, note that the leucocratic Bell Island pluton tonalites used as a starting material for model 1 lie along the trend defined by model 2 melts in figure 4. This suggests that late differentiates of the Bell Island pluton may be, at least in part, melts segregated from the system during reactive crystallization. All else being equal, such melts are more likely to be preserved than a melt separated under the precise conditions of the onset of hydration crystallization. It may be that this is why model 1, which does assume melt separation at the moment of hydration crystallization onset, ultimately fails to adequately reproduce the petrographic and petrologic characteristics of the pluton. Finally, note that batch separation and/or redistribution of evolved equilibrium melts may be important for understanding map-scale zoning in plutons.

ACKNOWLEDGMENTS

This article has benefited from the insightful reviews of two anonymous reviewers. This work was supported by National Science Foundation grants EAR-000719 (J. S. Beard) and EAR001004 (M. L. Crawford). Whole-rock chemical analyses were acquired, in part, by A. K. Sinha (Virginia Tech).

REFERENCES CITED

Beard, J. S., and Lofgren, G. E. 1991. Partial melting of basaltic and andesitic greenstones and amphibolites under dehydration melting and water-saturated conditions at 1, 3, and 6.9 kilobars. J. Petrol. 32:365–401.

Beard, J. S.; Ragland, P. C.; and Rushmer, T. 2004. Hydration crystallization reactions between anhydrous minerals and hydrous melt to yield amphibole and biotite in igneous rocks: description and implications. J. Geol. 112:617–621.

Bowen, N. L. 1928. The evolution of the igneous rocks. Princeton, NJ, Princeton University Press, 332 p.

Carr, M. 2003. Igpet for Windows, version 2003. Somerset, NJ, Terra Softa.

Cook, R. D. 1991. Mid-Cretaceous granitoids and orogeny in southern-most southeastern Alaska. PhD diss. Bryn Mawr College, Bryn Mawr, PA, 303 p.

Cook, R. D., and Crawford, M. L. 1994. Exhumation and tilting of the western metamorphic belt of the Coast orogen in southern southeastern Alaska. Tectonics 13: 528–537.

Crawford, M. L.; Hollister, L. S.; and Woodsworth, D. J. 1987. Crustal deformation and regional metamorphism across a terrane boundary, Coast Plutonic Complex, British Columbia. Tectonics 6:343–361.

Crawford, M. L.; Lindline, J.; Crawford, W. A.; and Sinha, A. K. 2002. Syntectonic tonalite magma emplacement during crustal thickening: the Bell Island Pluton, SE Alaska. Geol. Soc. Am. Abstr. Program 34:44.

Deer, W. A.; Howie, R. A.; and Zussman, J. 1963. Rock forming minerals. Vol. 2. Chain silicates. New York, Wiley, 379 p.

Drummond, M. S.; Ragland, P. C.; and Wesolowski, D. 1986. An example of trondhjemite genesis by means of alkali metasomatism: Rockford Granite, Alabama Appalachians. Contrib. Mineral. Petrol. 93:98–113.

Gehrels, G. E., and Berg, H. C. 1994. Geology of southeastern Alaska. *In* Plafker, G., and Berg, H. C., eds. The geology of Alaska. Boulder, CO, Geol. Soc. Am., p. 451–467.

Helz, R. T. 1981. Phase relations and compositions of amphiboles produced in studies of the melting behavior of rocks. *In* Veblen, D. R., and Ribbe, P. H., eds. Reviews in mineralogy. Vol. 9B. Amphiboles: petrology and experimental phase relations. Washington, DC, Mineral. Soc. Am., p. 279–353.

Leake, B. E. 1978. Nomenclature of amphiboles. Can. Mineral. 16:501–520.

Patino Douce, A. E., and Beard, J. S. 1995. Dehydration melting of biotite gneiss and quartz amphibolite from 3 to 15 kbar. J. Petrol. 36:707–738.

———. 1996. Effects of P, fO_2 and Mg/Fe ratio on dehydration-melting of model metagreywackes. J. Petrol. 37:999–1024.

Rapp, R. P. 1995. Amphibole-out phase boundary in partially melted metabasalt, its control over liquid fraction and composition, and source permeability. J. Geophys. Res. 100:15,601–15,610.

Rubin, C. M., and Saleeby, J. B. 2000. U-Pb geochronology of mid-Cretaceous and Tertiary plutons along the western edge of the Coast Mountains, Revillagigedo Island and Portland Peninsula, southeast Alaska. *In* Stowell, H. H., and McClelland, W. C., eds. Tectonics of the Coast Mountains, Southeastern Alaska and British Columbia. Geol. Soc. Am. Spec. Pap. 343:145–157.

Rushmer, T. 1991. Partial melting of two amphibolites: contrasting experimental results under fluid-absent conditions. Contrib. Mineral. Petrol. 107:41–59.

Sisson, T. W., and Grove, T. L. 1993. Experimental investigation of the role of H_2O in calc-alkaline differentiation and subduction zone magmatism. Contrib. Mineral. Petrol. 113:143–166.

Speer, A. L. 1984. Micas in igneous rocks. *In* Bailey, S. W., ed. Reviews in Mineralogy. Vol. 13. Micas. Washington, DC, Mineral. Soc. Am., p. 299–356.

Thomas, J. B.; Bodnar, R. J.; Shimizu, N.; and Sinha, A. K. 2002. Determination of zircon/melt partition coefficients from SIMS analysis of melt inclusions in zircon. Geochim. Cosmochim. Acta 66:2887–2901.

Thompson, A. B. 1982. Dehydration melting of pelitic rocks and the generation of H_2O-undersaturated granitic liquids. Am. J. Sci. 282:1567–1595.

Vielzeuf, D., and Schmidt, M. W. 2001. Melting relations in hydrous systems revisited: applications to metapelites, metagraywackes and metabasalts. Contrib. Mineral. Petrol. 41:251–267.

Wolf, M. B., and Wyllie, P. J. 1994. Dehydration melting of amphibolite at 10 kbar: the effects of temperature and time. Contrib. Mineral. Petrol. 115:369–383.